Royal Netherlands
Meteorological Institute
*Ministry of Infrastructure*
*and Water Management*

# PGV levels and location uncertainty for the Ekehaar 29-10-2023 event

E. Ruigrok, J. Spetzler, P. Kruiver and L. Evers

De Bilt, 2023 | Technical report; TR 411

Royal Netherlands
Meteorological Institute
*Ministry of Infrastructure*
*and Water Management*

# PGV levels and location uncertainty for the Ekehaar 29-10-2023 event

KNMI, R&D Seismology and Acoustics

November 9, 2023

## Introduction

The Ekehaar event on 29-10-2023:03:11:33.2 with a local magnitude of 2.20 was detected by the KNMI network (*KNMI*, 1993) and located near-real time with the Hypocenter method (*Lienert et al.*, 1986). This fast solution uses an average 1D model for the north of the Netherlands (*Kraaijpoel and Dost*, 2013). In this report, an updated location and its uncertainty is derived. Moreover, peak-ground velocity (PGV) levels are extracted from the recordings. These are used, together with a ground motion prediction equation, to find out where PGV levels of 2 mm/s and higher may have occurred.

## Epicenter

The epicenter is improved by using a best-fitting traveltime versus distance model based on a database of local P-wave traveltime picks. This data-driven model incorporates actual underburden velocities and only well pickable phase arrivals. An error estimate is derived from the spread in picking times from the best-fitting model. This error incorporates both the local variations of the velocity field as well as picking errors. These errors are propagated further into the epicentral probability density function (PDF). This results into an updated epicenter and its 95% confidence region. Details of the method are described in *Ruigrok et al.* (2023).

Fig. 1 shows the seismic sensors where manual P-wave picks are available. A grid search is performed for a region around the Hypocenter solution, as indicated by the red boxes in the figure. In the first step, equal differential time (EDT, *Zhou*, 1994) residuals are computed. That is, for each grid point and for each station combination, the traveltime differences are forward modelled and tabulated. From these values, the observed traveltime differences are subtracted to obtain the EDT residuals. In the second step, the PDF is derived from the EDT residuals, using a L1 norm (*Tarantola*, 2005). Fig. 2 shows the 95% confidence area of the resulting PDF. The locations with the maximum probability is assigned to be the updated epicenter.

The following list contains the new epicenter for the Ekehaar 29-10-2023 event, both in wgs84 coordinates and in the Dutch national triangulation system (RD). The line that surrounds the 95% confidence zone is by approximation an ellipse. The parameters of this ellipse (major axis, minor axis and orientation) are listed, together with the standard deviations describing the epicentral PDF in the direction with the largest uncertainty $\sigma_1$ and the perpendicular direction with the smallest uncertainty $\sigma_2$.

| |
|---|
| Epicenter in wgs84 [deg]: 6.5936, 52.9391 |
| Epicenter in RD [m]: 236100, 550900 |
| Depth [km]: 3.4 |
| Ellipse major and minor axes [m]: 1372, 1136 |
| $\sigma_1$ and $\sigma_2$ [m]: 280, 232 |
| Orientation of the major axis [deg]: 136 |

The waveform data used in the above analysis is publicly available and can be obtained through:

**GUI:** `http://rdsa.knmi.nl/dataportal/`

**FDSN webservices:** `http://rdsa.knmi.nl/fdsnws/dataselect/1/`

## Depth

For estimating event depth, local velocity profiles are needed. A P-wave profile is extracted from the Netherlands-wide model DGM-deep (*Van Dalfsen et al.*, 2006) at the location of the initial epicenter (Fig. 3). The S-wave profile is obtained by using Vp/Vs ratio's from the different lithologies as estimated in *Romijn* (2017) from P- and S-wave logging. For the depth estimation only five nearby sensors are used: ELE, ASS1, ASS2, VRS and ENV4. For these sensors, the velocity profiles are approximately valid and arrival times can be modeled quite accurately using finite differences. At the three nearest stations, also the onset of the direct S-wave is picked. The S-P delay times are inverted together with the P-EDT times to obtain an estimate of the depth. The resulting 95% confidence zone is shown in Fig. 4, yielding a most-likely source location at 3.4 km depth. This is just below the gas-water contact of Eleveld, which is at approximately 3.3 km depth (www.nlog.nl).

## PGV levels

For induced events outside Groningen, the protocol as established in *Ruigrok and Dost* (2020) is used to compute PGV[1] contours. From the spatial distribution of PGV, contours are extracted for the P50, P90 and P99 probabilities. The P50 is the average field, which thus has a 50% probability of exceedance. The P90 is the 90th percentile, which PGV field has a 10% probability of exceedance. The P99 has a 1% probability of exceedance.

The PGV field is a combination of a model and local recordings. The model BMR2 (*Ruigrok and Dost*, 2020) is used. This is a ground motion prediction equation that provides the PGV level and its variability as a function of magnitude, epicentral distance and depth of the event. The model has been calibrated with PGV recordings from induced events in the Netherlands. Recordings at the Earth's surface from one specific event are used to estimate how much stronger, or weaker, this event is with respect to the average event in the database. This yields the so-called event term, which is used to adapt the model with a distance-independent shift up-, or downwards. Still, uncertainty exists of the actual PGV that materialized at a certain location. This so-called within-event variability is caused, e.g., by the radiation pattern of the source and variations in near-surface amplification. At and nearby places where the PGV has been recorded, the uncertainty of the PGV is reduced by blending the model with the actually measured PGV. If the combined field reaches levels of 2 mm/s and higher, PGV contours are extracted and shown on a map.

All accelerometer recordings at distances smaller than 70 km are evaluated, which yields 39

[1] In this report, as PGV measure we use 'PGVrot', which is defined as $max(\sqrt{u_E^2(t) + u_N^2(t)})$, where $u_E(t)$ and $u_N(t)$ are the particle-velocity recording on the East and North component, respectively.

recordings with a signal-to-noise ratio larger or equal to 6 dB. The nearest and furthest accepted stations are at 2.24 and 43.06 km epicentral distance, respectively. Table 1 lists the PGV values, with the largest value being 1.412 mm/s. Fig. 5 shows these recorded PGV values as function of epicentral distance, together with the event-term shifted BMR2 model for $M$=2.20. As hypocenter depth, 3.4 km is used (Fig. 4).

Using the 39 recordings results in an event term of -0.357. This is the average difference between recorded and modeled PGV levels (expressed in natural log). With the event term quantified, the remaining model variability is the within-event variability $\phi = 0.536$. This remaining variability is implemented to yield the confidence regions as plotted in Fig. 5. This figure shows that the P50 field does not reach the 2 mm/s threshold level, but the P90 and P99 fields do.

The radially-symmetrical PGV fields (Fig. 5) are locally corrected with the recorded PGV levels (Table 1) to obtain estimates of the PGV distribution over the Earth's surface. The best estimate (P50 field) does not reach 2 mm/s. For the P90 field (10% chance of exceedance) an area remains where the 2 mm/s threshold level is exceeded (Fig. 6). For the P99 field (1% chance of exceedance) an area remains where the 3 mm/s threshold level is exceeded (Fig. 7). The gridded versions of the contours are available as kml files.

| **Station name** | **Epicentral distance [km]** | **PGV [mm/s]** |
|---|---|---|
| ELE | 2.23 | 1.412 |
| ASS1 | 4.94 | 0.643 |
| ASS2 | 8.51 | 0.088 |
| VRS | 10.81 | 0.068 |
| N020 | 17.53 | 0.052 |
| ZDL | 17.20 | 0.079 |
| DON | 18.27 | 0.027 |
| DR030 | 19.67 | 0.018 |
| DVR | 21.41 | 0.010 |
| EVK | 21.39 | 0.067 |
| VDM20 | 22.79 | 0.027 |
| G540 | 23.35 | 0.022 |
| WPS | 25.77 | 0.011 |
| VNDM0 | 25.55 | 0.031 |
| OOTH | 25.66 | 0.013 |
| G660 | 26.74 | 0.017 |
| DR020 | 26.83 | 0.014 |
| G490 | 27.95 | 0.025 |
| G550 | 28.31 | 0.019 |
| FDKD | 29.60 | 0.009 |
| WSVN | 29.63 | 0.080 |
| G380 | 29.24 | 0.022 |
| ODBK | 30.81 | 0.007 |
| BFB2 | 29.93 | 0.021 |
| G440 | 30.10 | 0.018 |
| G500 | 29.90 | 0.023 |
| COE3 | 30.15 | 0.015 |
| UTRP | 32.53 | 0.023 |
| MAR | 32.55 | 0.013 |
| G390 | 33.01 | 0.013 |
| G590 | 32.90 | 0.020 |
| G570 | 36.02 | 0.013 |
| G340 | 36.70 | 0.033 |
| G470 | 36.87 | 0.032 |
| G410 | 37.39 | 0.013 |
| G280 | 38.15 | 0.018 |
| G480 | 40.88 | 0.017 |
| G420 | 41.05 | 0.027 |
| G640 | 43.17 | 0.014 |

Table 1: Recorded PGVs

## Discussion and Conclusions

The epicenter of the M2.2 Ekehaar event maps to the southern part of the Eleveld gasfield. The updated location is about 800 m east of the fast Hypocenter solution (Fig. 2). As a most-likely depth, 3.4 km is found (Fig. 4), which is just below the gas-water contact. This year the M2.2 Ekehaar event is the third located earthquake with an epicenter at Eleveld. The two previous events were the Hooghalen M1.9 (*Ruigrok and Kruiver*, 2023) and the Ekehaar M1.3 events. All three events occurred in October 2023. The first event was at the western bounding fault of Eleveld, the second event has a most likely epicenter shifted about 600 m to the east. The third event, the one analysed in this report, has an epicenter that is shifted again about 1000 m further to the east. No other seismic events were detected at Eleveld since a sequence of events in 2014.

For the Ekehaar 29-10-2023 event, the highest recorded PGV is 1.412 mm/s at station ELE. A ground-motion prediction equation and the measured PGV values have been used to compute the PGV fields that have a 50%, a 10% and a 1% chance of exceedance. The P50 field stays below 2 mm/s, the P90 field reaches levels between 2 and 3 mm/s in the epicentral area and the P99 PGV field reaches levels between 3 and 4 mm/s near the epicenter.

# References


KNMI (1993), Netherlands Seismic and Acoustic Network, Royal Netherlands Meteorological Institute (KNMI), Other/Seismic Network, https://doi.org/10.21944/e970fd34-23b9-3411-b366-e4f72877d2c5.

Kraaijpoel, D., and B. Dost (2013), Implications of salt-related propagation and mode conversion effects on the analysis of induced seismicity, *Journal of Seismology*, *17*(1), 95–107.

Lienert, B. R., E. Berg, and L. N. Frazer (1986), HYPOCENTER: An earthquake location method using centered, scaled, and adaptively damped least squares, *Bulletin of the Seismological Society of America*, *76*(3), 771–783.

Romijn, R. (2017), Groningen velocity model 2017, *Tech. rep.*, NAM (Nederlands Aardolie Maatschappij), https://nam-feitenencijfers.data-app.nl/download/rapport/9a5751d9-2ff5-4b6a-9c25-e37e76976bc1?open=true.

Ruigrok, E., and B. Dost (2020), Advice on the computation of peak-ground-velocity confidence regions for events in gas fields other than the Groningen gas field, *KNMI Technical Report*, *TR-386*, https://cdn.knmi.nl/knmi/pdf/bibliotheek/knmipubTR/TR386.pdf.

Ruigrok, E., and P. Kruiver (2023), PGV levels and location uncertainty for the Hooghalen 01-10-2023 event, *KNMI Technical Report*, *TR-409*, https://www.knmi.nl/research/publications/pgv-levels-and-location-uncertainty-for-the-hooghalen-01-10-2023-event.

Ruigrok, E., P. Kruiver, and B. Dost (2023), Construction of earthquake location uncertainty maps for the Netherlands, *KNMI Technical Report*, *TR-405*, https://cdn.knmi.nl/knmi/pdf/bibliotheek/knmipubTR/TR405.pdf.

Tarantola, A. (2005), *Inverse Problem Theory and Methods for Model Parameter Estimation*, SIAM, Philadelphia.

Van Dalfsen, W., J. Doornenbal, S. Dortland, and J. Gunnink (2006), A comprehensive seismic velocity model for the netherlands based on lithostratigraphic layers, *Netherlands Journal of Geosciences*, *85*(4), 277.

Zhou, H.-w. (1994), Rapid three-dimensional hypocentral determination using a master station method, *Journal of Geophysical Research: Solid Earth*, *99*(B8), 15,439–15,455.

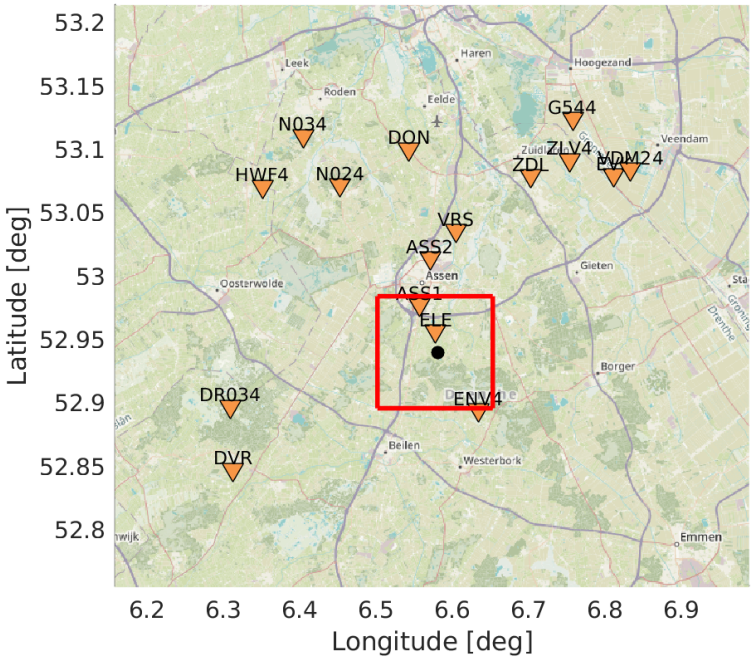


Figure 1: Overview map with locations of stations (orange triangles) where P-wave onsets were picked, the fast Hypocenter solution (black dot) and the boundary line of the area in which a grid search is done (red box). Background map is from www.openstreetmap.org.

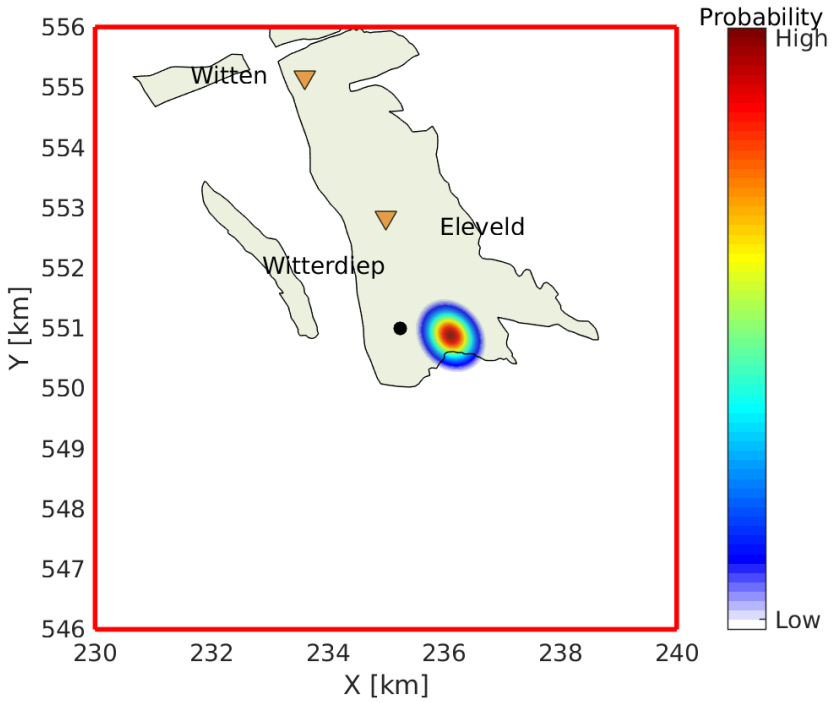


Figure 2: Map showing hydrocarbon fields (green-filled polygons), the fast Hypocenter solution (black dot) and the epicentral probability density function (PDF) using time-differences and an optimized model. The 95% confidence area of the PDF is shown. The field polygons are from www.nlog.nl, using the March 2023 update.

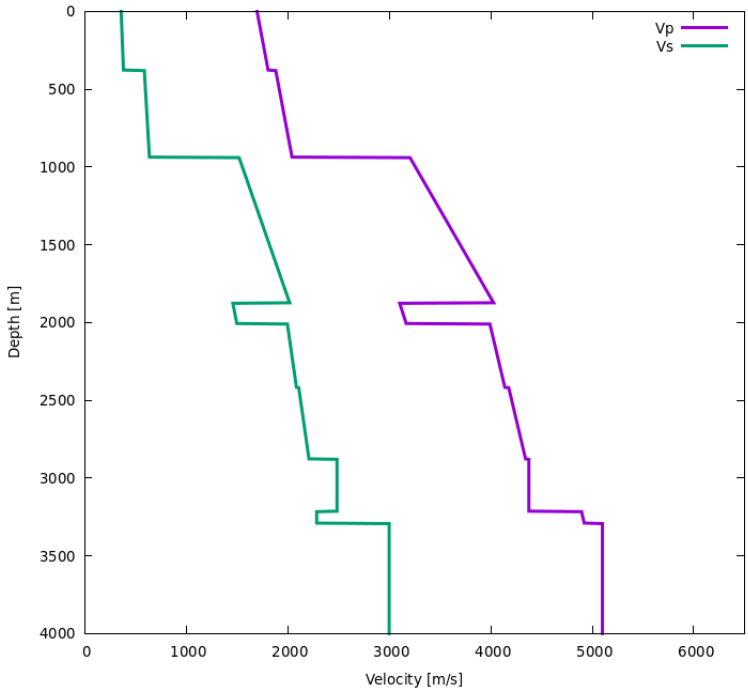


Figure 3: The P-wave (purple line) and S-wave (green line) velocity model used for estimating the depth of the event. The velocity model has been derived from DGM-deep ( *Van Dalfsen et al.*, 2006).

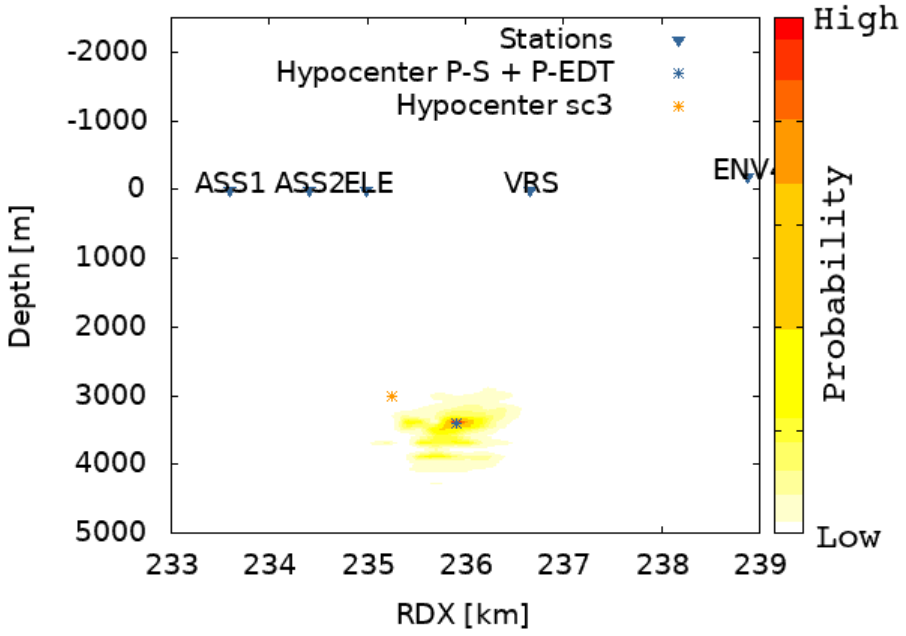


Figure 4: A depth slice through the 95% confidence zone that is obtained by using P-EDT and S-P delay times at five nearby stations. For induced events, the default depth for the fast Hypocenter method (labeled 'Hypocenter sc3' in the figure) is 3.0 km. The updated depth is 3.4 km (blue star).

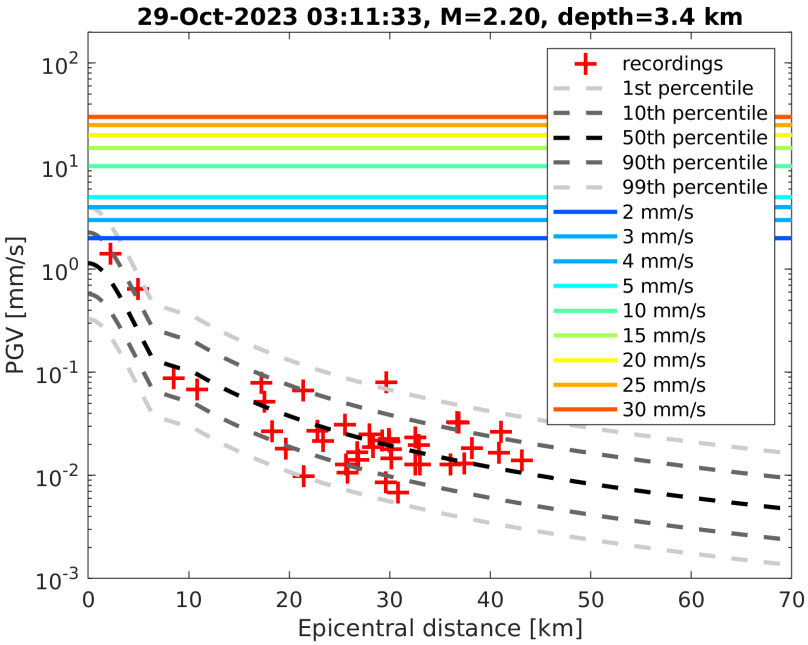


Figure 5: BMR2 model and confidence regions for this model (dashed lines), PGV thresholds (coloured lines) and measured PGV values for the Ekehaar event (red crosses). Both the model and the recordings are expressed in PGVrot.

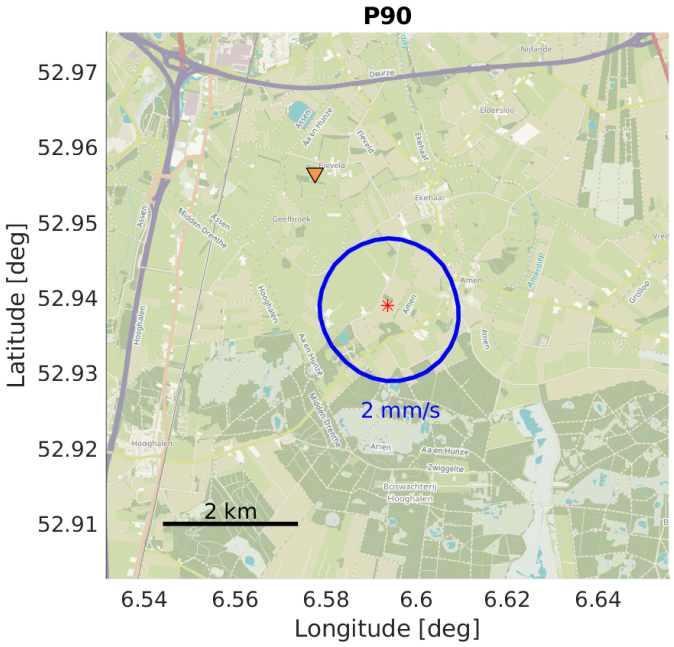


Figure 6: The bounding line of the 2 mm/s PGV threshold region for the P90 model (blue line), and the updated epicenter (red star), together with the nearest accelerometer (ELE, orange triangle).

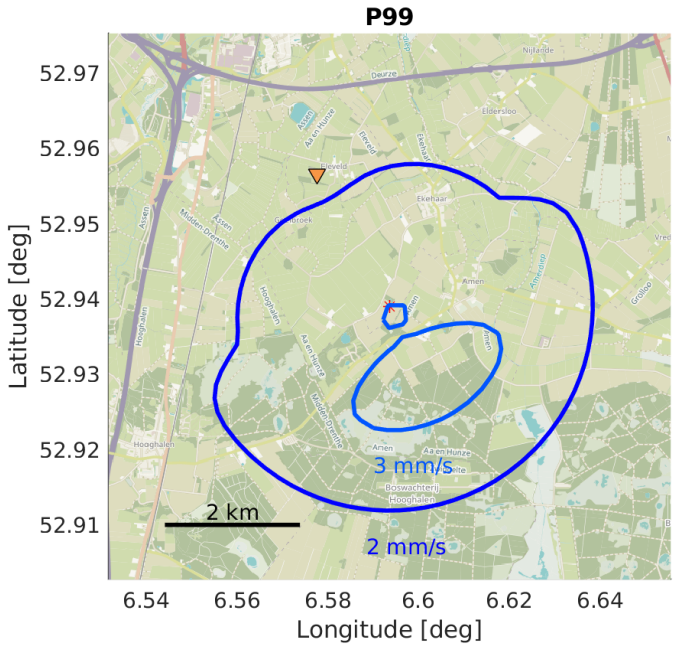


Figure 7: The bounding lines of the 2 mm/s and 3 mm/s PGV threshold regions for the P99 model, and the updated epicenter (red star), together with the nearest accelerometer (ELE, orange triangle).

**Royal Netherlands Meteorological Institute**

PO Box 201 | NL-3730 AE De Bilt
Netherlands | www.knmi.nl